Ratiometric Luminescent Detection of Bacterial Spores with Terbium Chelated Semiconducting Polymer Dots

ARTICLE *in* ANALYTICAL CHEMISTRY · AUGUST 2013

Impact Factor: 5.64 · DOI: 10.1021/ac4016616 · Source: PubMed

7 AUTHORS, INCLUDING:

Kaiwen Chang
Jilin University
8 PUBLICATIONS **25** CITATIONS

SEE PROFILE

Weiping Qin
Jilin University
360 PUBLICATIONS **4,538** CITATIONS

SEE PROFILE

analytical chemistry

Article

pubs.acs.org/ac

Ratiometric Luminescent Detection of Bacterial Spores with Terbium Chelated Semiconducting Polymer Dots

Qiong Li,[†] Kai Sun,[†] Kaiwen Chang,[†] Jiangbo Yu,[‡] Daniel T. Chiu,[‡] Changfeng Wu,*[,†] and Weiping Qin*[,†]

[†]State Key Laboratory on Integrated Optoelectronics, College of Electronic Science and Engineering, Jilin University, Changchun, Jilin 130012, China

[‡]Department of Chemistry, University of Washington, Seattle, Washington 98195, United States

ABSTRACT: We report a ratiometric fluorescent sensor based on semiconducting polymer dots chelated with terbium ions to detect bacterial spores in aqueous solution. Fluorescent polyfluorene (PFO) dots serve as a scaffold to coordinate with lanthanide ions that can be sensitized by calcium dipicolinate (CaDPA), an important biomarker of bacterial spores. The absorption band of PFO dots extends to deep UV region, allowing both the reference and the sensitizer can be excited with a single wavelength (~275 nm). The fluorescence of PFO remains constant as a reference, while the Tb^{3+} ions exhibit enhanced luminescence upon binding with DPA. The sharp fluorescence peaks of β-phase PFO dots and the narrow-band emissions of Tb^{3+} ions enable ratiometric and sensitive CaDPA detection with a linear response over nanomolar concentration and a detection limit of ~0.2 nM. The Pdots based sensor also show excellent selectivity to CaDPA over other aromatic ligands. Our results indicate that the Tb^{3+} chelated Pdots sensor is promising for sensitive and rapid detection of bacterial spores.

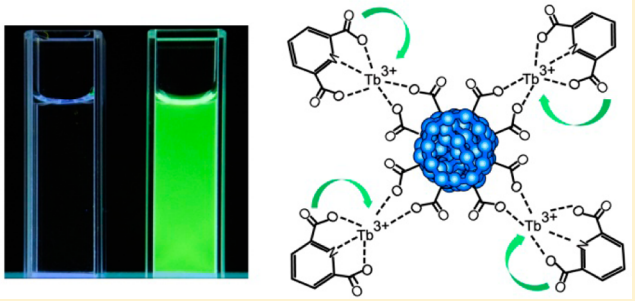

Bacterial spores are very resistant microbial structures toward environmental extremes. The spores can survive even when the bacteria were killed and will germinate when conditions are right. Therefore, detecting bacterial spores and determining their concentration are very useful in many applications. For example, public health workers could rapidly monitor indoor environments, water, or food quality. Some spores, such as *Bacillus anthracis* spores, are extremely hazardous to human beings and animals.[1] In the most ominous application, *Bacillus anthracis* spores have been used as delivery vehicles in biological warfare and bioterrorism.[2] Accordingly, accurate and sensitive detection of anthrax spores is important for preventing the biological attack and outbreak of the disease. During the past decades, a number of methods have been developed for the detection of bacillus spores, including important biological methods such as immunoassays and polymerase chain reactions (PCRs).[3,4] The biological methods generally require expensive reagents and considerable sample processing prior to analysis. Recently, optical methods for bacterial spore detection have attracted a great deal of interest. For example, surface enhanced Raman spectroscopy (SERS) provides effective detection of bacillus spores with the limit of detection (LOD) of ~2.6×10^3 spores, well below the anthrax infectious dose of 10^4 spores.[5,6] Compared to SERS, luminescence techniques are capable of rapid, sensitive, and selective detection of bacillus spores with a low level of detection limit.[6−14]

The optical methods including SERS and luminescence techniques are primarily based on detection of calcium dipicolinate (CaDPA), an important biomarker and major constituent of bacterial spores, which accounts for about 10% of the dry weight and can be released into bulk solution by physical lysis, chemical lysis, or germination.[1,15,16] High affinity binding of DPA to lanthanide ions (Ln^{3+}) enables very sensitive assays for bacterial spore detection with unique features such as bright Ln^{3+} luminescence, long lifetime, and high enhancement ratio upon DPA sensitization compared to free Ln^{3+} ions.[7,9−11,17,18] Different platforms containing lanthanide ions have been developed, including solid films,[6,19] carbon nanotubes,[12] nanoparticles,[10] and metal organic frameworks (MOF).[14] These luminescent sensors show LODs varying from subnanomolar to a few tens of nanomolar of DPA, mainly because of different optical systems and detectors of instruments employed in different groups. In addition, most of the lanthanide based sensors measure the concentration of CaDPA by the change of fluorescence intensity alone, therefore encountering inevitable challenges induced by intensity fluctuations due to instrumental or environmental factors, especially at very low CaDPA concentrations. This problem can be overcome by ratiometric fluorescent detection because it measures the relative changes of fluorescence intensities at two

Received: June 4, 2013
Accepted: August 22, 2013
Published: August 22, 2013

different wavelengths.[6,19] The absolute concentration of an analyte can be quantitatively determined by the self-calibration curve of the ratiometric sensor.

Semiconducting polymer dots (Pdots) have recently received considerable attention for their high fluorescence brightness, excellent photostability, and nontoxic characteristics.[20−26] Very recently, we have developed methods for surface functionalization and bioconjugation and demonstrated the applications of Pdot-bioconjugates in specific cellular labeling and in vivo targeting.[25,27,28] Successful functionalization also allows for covalent attachment of fluorescent dyes to develop a variety of Pdot sensors for pH or temperature measurements in cellular environment.[29,30] In another aspect, the surface functional molecules have been used to coordinate with metal ions, forming Pdot ion sensors to detect environmentally relevant ions, such as Cu^{2+} and Hg^{2+}.[31,32]

On the basis of these studies, this article presents a Pdot platform for the ratiometric detection of the biomarker CaDPA of bacterial spores with high sensitivity and selectivity. We employed a highly fluorescent semiconducting polymer polyfluorene (PFO) to form Pdots with surface carboxyl groups that can coordinate with Tb^{3+} ions. Because the absorption band of Pdots extends to the deep UV region, the Pdot reference and DPA sensitized Ln^{3+} ions can be excited with a single wavelength (~275 nm). The fluorescence of Pdots remains unchanged as a reference, while the Tb^{3+} ions exhibit enhanced luminescence upon binding with DPA. The sharp fluorescence peaks of β-phase PFO dots and the narrow-band emissions of Tb^{3+} ions enable ratiometric DPA detection with a linear response over the nanomolar concentration range and a detection limit of 0.2 nM.

EXPERIMENTAL SECTION

Materials. Fluorescent semiconducting polymer poly(9,9-dioctylfluorene) (PFO, MW 146 000, polydispersity 2.3) was purchased from ADS Dyes, Inc. (Quebec, Canada). Terbium(III) chloride hexahydrate ($TbCl_3 \cdot 6H_2O$) was purchased from Shanghai Shabo Chemical Technology, Inc. Dipicolinic acid (DPA) was purchased from J&K Chemical Ltd. (Beijing, China). The functional copolymer poly(styrene-*co*-maleic anhydride) (PSMA, average M_n ~1 700, styrene content 68%) and other materials were purchased from Sigma-Aldrich (St. Louis, MO).

Preparation of Pdots. Functionalized Pdots were prepared by using the nanoprecipitation method as described previously.[20,33,34] First, semiconducting polymer PFO and functional polymer PSMA were dissolved in tetrahydrofuran (THF) to make stock solutions with a concentration of 1 mg/mL, respectively. PFO and PSMA were mixed and diluted with THF to produce a solution mixture with a PFO concentration of 50 μg/mL and a PSMA concentration of 10 μg/mL. The mixture was sonicated to form a homogeneous solution. A 5-mL quantity of the solution mixture was added quickly to 10 mL of Milli-Q water in a bath sonicator. THF was removed by nitrogen stripping, followed by filtration through a 0.2 μm filter. The resulting functionalized Pdot dispersions are clear and stable for months without signs of aggregation.

Preparation of CaDPA. CaDPA powder was prepared by the neutralizing reaction. A 3.3-mmol quantity of the DPA and an equal molar amount of $Ca(OH)_2$ were separately dissolved in 50 mL of Milli-Q water. Then the DPA solution was neutralized by dropwise addition of $Ca(OH)_2$ aqueous solution. The reaction solution was stored at 5 °C for 48 h, followed by filtration and evaporation.

Characterizations of the Sensor. For the sensor for CaDPA detection, terbium chloride (0.1 mM $TbCl_3$) was added to an aqueous solution of functionalized PFO dots to produce a solution with a Pdot concentration of about 80 pM and terbium concentration of 1 μM, respectively. The above solution was agitated for 5 min. Then luminescence sensing experiments of the terbium chelated PFO dots were performed by adding different volumes of CaDPA (0.1 μM) to the terbium chelated Pdots solutions. The nanoparticle size was measured by dynamic light scattering (DLS, Malvern Zetasizer NanoZS). UV−vis absorption spectra were recorded on a Shimadzu UV-2550 scanning spectrophotometer using a 1 cm quartz cuvette. Fluorescence spectra were measured on a Hitachi F-4500 fluorescence spectrometer.

RESULTS AND DISCUSSION

Our strategy for detecting CaDPA was described in Scheme 1. A fluorescent semiconducting polymer poly(9,9-dioctylfluorene) (PFO) and a functional polymer poly(styrene-*co*-maleic anhydride) (PSMA) were employed to prepare functionalized PFO dots. Hydrolysis of each maleic anhydride unit in PSMA results in two closely spaced carboxyl groups, which were known to have high binding affinity with lanthanide ions such as Tb^{3+}.[35] Indeed, when mixing Tb^{3+} ions at a millimolar concentration with PFO dots at tens of nanomolar, the coordination of Tb^{3+} ions with carboxyl groups can cause aggregation of the Pdots. However, the concentrations of Tb^{3+} and Pdots employed in this assay were less than 1 μM and 100 pM, respectively, several orders of magnitude lower than the aggregation concentrations. As shown by the dynamic light scattering measurements in Figure 1A−C, the Pdot solutions (100 pM) in the presence of Tb^{3+} ions (1 μM) and/or the CaDPA analyte (100 nM) show particle size distribution comparable to that of the Pdots alone. The above solutions are stable for months without sign of aggregation, indicating good colloidal stability in our experimental concentration range.

Scheme 1. Ratiometric Detection of CaDPA with Terbium Chelated PFO Dots[a]

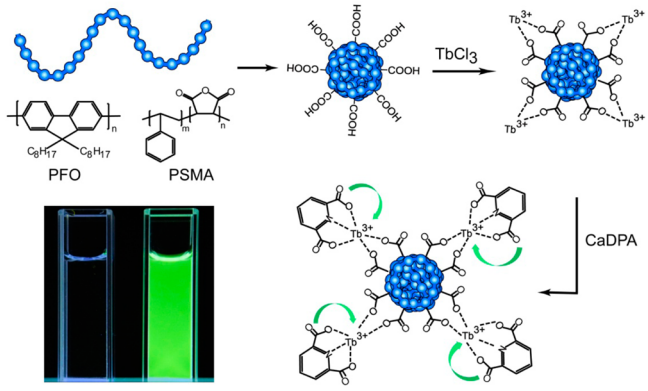

[a]PFO dots were functionalized with surface carboxyl groups that were chelated with terbium ions. When coordinating with Tb^{3+} ions, DPA serves as antennas to absorb light and sensitize the Tb^{3+} luminescence. The PFO dots were used as a scaffold and reference because its blue fluorescence remains constant in the sensor. The picture shows a clear color change at 0.5 μM CaDPA concentration, which can be identified by unaided eyes under a UV-lamp illumination.

dx.doi.org/10.1021/ac4016616 | Anal. Chem. 2013, 85, 9087−9091

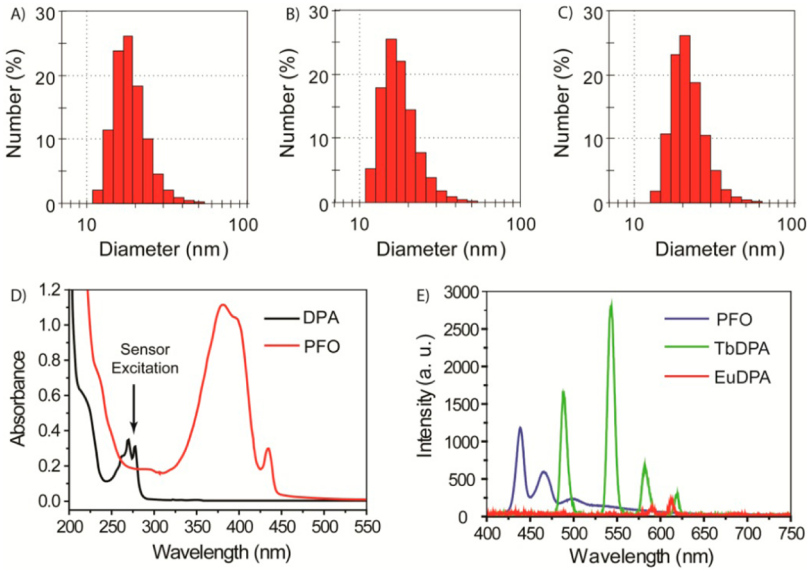

Figure 1. Characterization of the CaDPA sensor. (A) Size distribution of the PFO dots alone measured by dynamic light scattering; (B) size distribution of the Tb^{3+} chelated PFO dots; (C) size distribution of the Tb^{3+} chelated PFO dots in presence of CaDPA. (D) Absorption spectra of the PFO dots and DPA. As indicated by the arrow, both PFO dots and DPA ligand can be excited at the wavelength of 275 nm. (E) Emission spectra of the PFO dots, Tb−DPA, Eu−DPA complexes. The sensitized luminescence of Tb^{3+} ions is about 10 times higher than that of the Eu^{3+} at the same concentration of DPA ligand.

The semiconducting polymer PFO was selected because its broad absorption band extends to the deep UV region which matches the absorption peak (~275 nm) of CaDPA (Figure 1D). The PFO dots and Tb−DPA complex can be simultaneously excited at one wavelength at 275 nm, but their luminescence does not affect each other. In addition, *β*-phase PFO dots prepared by the reprecipitation method exhibit narrow and sharp fluorescence peaks in aqueous solution (shown in Figure 1E),[36] so the PFO dots can be used as a good reference. In contrast, most fluorescent dyes absorbing in the deep UV region are not water-soluble. In addition, fluorescent dyes generally have small Stokes shift, which makes it difficult to separate the emission from the excitation light. The luminescence of lanthanide ions arises from parity forbidden 4f−4f transitions that typically exhibit very low extinction coefficients (1−10 M^{-1} cm^{-1}). The extinction coefficients can be effectively increased by the well-known "antenna effect", whereby organic chromophores coordinated with lanthanide ions serve as antennas to absorb light and then transfer energy to the metal ions. In this study, Tb^{3+} was selected for DPA detection because it has a more sensitive and intense luminescence response upon coordination with DPA than Eu^{3+} at a given DPA concentration and excitation intensity. Many previous reports described Eu^{3+} based DPA detection, rather than using Tb^{3+} ions, because of the concern that the second-order scattering peak of the 275 nm excitation interferes with the 544 nm emission of the Tb^{3+} ion.[10,13] However, the interference can be eliminated by placing a long-pass filter in front of the detector. As shown in Figure 1E, the Tb^{3+}−DPA complex shows characteristic emission peaks of Tb^{3+} ions ($^5D_4$−^7F_J transitions, J = 6, 5, 4, and 3), without any interference from the 275 nm excitation. Under the same excitation and detection conditions, the Tb^{3+}−DPA complex at the same concentration shows the emission intensity an order of magnitude higher than that of the Eu^{3+}−DPA complex (Figure 1E). Therefore, this study employs the Tb^{3+} ions and the PFO dots to construct the ratiometric sensor.

The chelation of the Tb^{3+} ions on the Pdot surface is a useful step to improve the sensor performance as compared to a mixture of free Pdots and Tb ions. In an aqueous solution containing only Tb^{3+} ions, the Tb^{3+} ions exist in the form of [Tb−H_2O] complexes. In the presence of CaDPA, DPA replaces part of the water molecules and forms the [H_2O−Tb-DPA] complexes. At low DPA concentrations, water molecules can still coordinate with Tb^{3+} ions and the hydroxyl groups significantly quench the Tb^{3+} luminescence. When the Tb^{3+} ions were chelated on the Pdot surface, the nanopartice can exclude water molecules from the coordination sphere through the formation of the [Pdot−Tb−DPA] complex, which can minimize the nonradiative quenching of the Tb^{3+} emission, resulting in an increase in the overall quantum yield and thereby affording a corresponding improvement in the detection sensitivity for CaDPA.

Fluorescence titrations were performed to evaluate the sensitivity of the CaDPA sensor. Figure 2 shows the luminescence response of the sensor as CaDPA was introduced into the aqueous system when excited at 275 nm. As seen from the figure, the emission spectrum of the sensor prior to DPA addition was dominated by the PFO dots, with the major emission peak at 439 nm and a well resolved vibronic structure in agreement with those of the pure Pdot solution (Figure 1E). A very weak emission peak at 544 nm in absence of CaDPA is due to the direct excitation of the Tb^{3+} ions (the inset of Figure 2). Addition of small aliquots of CaDPA solution enhances the emission intensities of the Tb^{3+} ions due to efficient energy transfer from the DPA ligands to the Tb^{3+} ions. The emission peaks at 490 nm, 544 nm, 585 nm, and 619 nm are attributed to the characteristic transitions of the Tb^{3+} ions, from $^5D_4$ energy level to ^7F_J multiplets (J = 6, 5, 4, and 3), respectively. The inset in Figure 2 clearly shows the luminescence spectra with increasing the CaDPA concentration from 0 nM to 4 nM. As clearly indicated by the spectra, the Tb^{3+} emission intensity at 544 nm jumps noticeably upon the first addition of CaDPA, which corresponds to a concentration of 0.2 nM. Such a

dx.doi.org/10.1021/ac4016616 | *Anal. Chem.* 2013, 85, 9087−9091

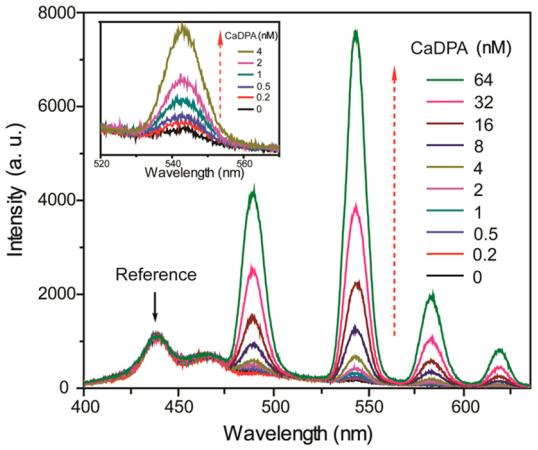

Figure 2. Luminescence spectra of the Tb^{3+} chelated PFO dots with increasing CaDPA concentration. All the spectra were measured with an excitation of 275 nm under the same experimental conditions. The inset shows the luminescence changes with the CaDPA concentration from 0 to 4 nM.

detection limit is 6 orders of magnitude lower than an infectious dosage of the spores (6×10^{-5} M required).[7,8] The emission intensity at 544 nm was greatly enhanced upon further increasing the CaDPA concentration from subnanomolar to tens of nanomolar. Under the same excitation and detection conditions, the detector of our fluorometer was saturated at the concentration of 100 nM CaDPA. As shown in Figure 3A, the Tb^{3+} emission changes linearly with CaDPA in this concentration range and the detection range can be increased by adjusting the sensor concentration. Interestingly, the CaDPA sensing and the concomitant luminescent changes were clearly visible under a UV-lamp illumination, where the weak blue luminescence of the sensor solution turned green upon addition of CaDPA. In this case, a color change can be identified by unaided eyes, even at a CaDPA concentration as low as 0.5 μM.

As a significant feature, the sensors exhibit constant blue fluorescence at 439 nm from PFO and sensitive green emission at 544 nm due to coordination of Tb^{3+} with DPA ligands. Both the two emission peaks are narrow and sharp, therefore forming excellent ratiometric measurements on CaDPA concentration. On the basis of the luminescence spectra, the intensity ratio of the 544 nm peak to 439 nm peak was plotted as a function of the CaDPA concentration (Figure 3B). On the basis of this curve, the sensor shows a change of ~11% per nanomolar CaDPA, and a linear relationship with $R^2 = 0.999$ exists in our experimental concentration range from 0.2 nM to 64 nM. The sensitivity and limit of detection (0.2 nM) of the Pdot based sensor are among the best performance reported so far.[5,6,9,37] More importantly, the ratiometric sensing capability provided by this sensor is useful for quantitative determination CaDPA concentration, not affected by intensity fluctuations due to instrumental or environmental factors.

Selectivity is a critical parameter to evaluate the performance of a fluorescent sensor. We further investigated the selectivity of the Pdot sensor for CaDPA versus several aromatic ligands including benzoic acid, *m*-phthalic acid, *o*-phthalic acid, 1,3,5-trimesic acid, and three amino acids such as D-phenylalanine, D-aspartic acid, and glutamic acid. All these compounds contain carboxylic acid groups and might coordinate with Tb^{3+} ions. In addition, the three amino acids represent important compositions that are abundantly present in many bacterial spores.[38] The excellent selectivity of Pdot sensor for DPA over other components was shown in Figure 4. At the same concentration, only CaDPA induced a prominent luminescence enhancement, and the other components resulted in very little fluorescent changes almost negligible compared to CaDPA. These results indicate that the Tb^{3+} chelated Pdots sensor is selective for

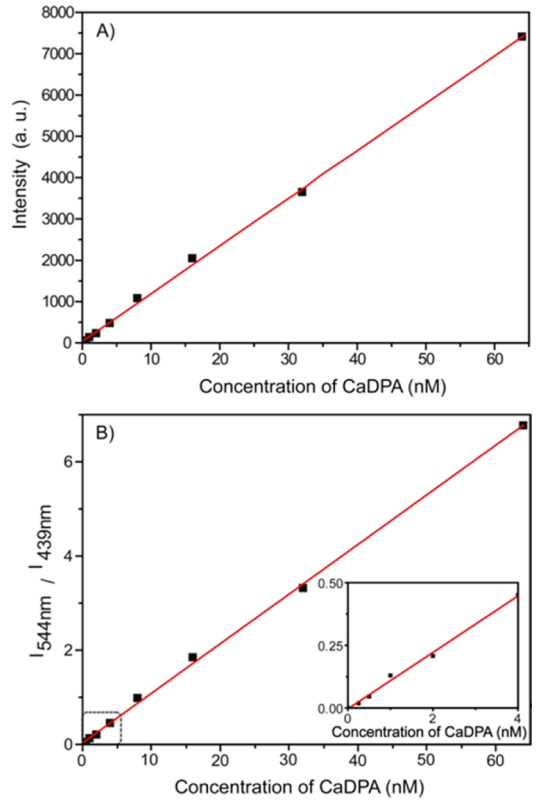

Figure 3. (A) Plot of luminescence intensity change (544 nm) of the Pdots sensor with increasing CaDPA concentration; (B) ratiometric calibration plot (I_{544}/I_{439}) of the Pdot sensor as a function of CaDPA concentration. The inset shows the magnified curve in the low concentration range from 0 nM to 4 nM. The scattered squares are experimental data, and the solid curves are linear fits with $R_A^2 = 0.999$ and $R_B^2 = 0.999$, respectively.

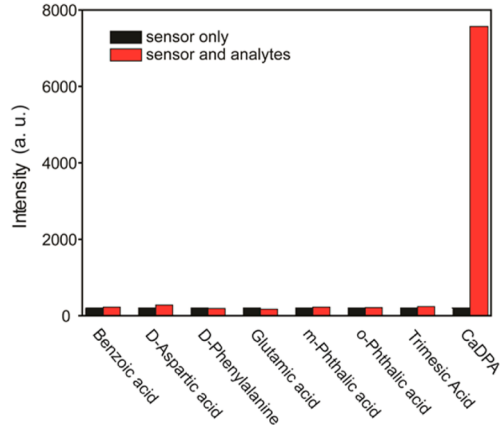

Figure 4. Selectivity of the terbium chelated Pdot sensor for CaDPA over several aromatic ligands and amino acids. The concentrations of all the compounds are the same (64 nM), and measurements are performed under identical conditions.

dx.doi.org/10.1021/ac4016616 | *Anal. Chem.* 2013, 85, 9087−9091

efficient recognition of *Bacillus anthracis* spores. Finally, rapid detection of hazardous spores such as *Bacillus anthracis* spores is also important because inhalation of more than 10^4 *Bacillus anthracis* spores can lead to death in 24−48 h without medical attention. The Pdot sensor shows quick response upon introducing an aliquot of CaDPA (64 nM) to the sensor solution. The luminescence from Tb^{3+} ions rapidly increases in a few seconds and then reaches a stable stage in tens of seconds, thus enabling a rapid detection of bacterial spores.

CONCLUSION

In summary, a ratiometric Pdot sensor was constructed to detect CaDPA, an important biomarker of bacterial spores. Carboxyl functionalized PFO dots serve as a scaffold to coordinate with Tb^{3+} ion. The fluorescence of Pdots remains constant as a reference, and the luminescence from Tb^{3+} ions is greatly enhanced upon binding with DPA, therefore forming ratiometric CaDPA detection. The sensor shows excellent sensitivity and selectivity with a limit of detection of 0.2 nM, among the best performance of various CaDPA sensors reported so far. This study provides a promising platform for sensitive and rapid detection of bacterial spores.

AUTHOR INFORMATION

Corresponding Authors

*E-mail: cwu@jlu.edu.cn.
*E-mail: wpqin@jlu.edu.cn.

Notes

The authors declare no competing financial interest.

ACKNOWLEDGMENTS

We acknowledge financial support from "Thousand Talents Program" and the National Science Foundation of China (Grant No. 61222508).

REFERENCES

(1) Walt, D. R.; Franz, D. R. *Anal. Chem.* **2000**, *72*, 738A−746A.
(2) Shabani, A.; Marquette, C. A.; Mandeville, R.; Lawrence, M. F. *Analyst* **2013**, *138*, 1434−1440.
(3) Hurtle, W.; Bode, E.; Kulesh, D. A.; Kaplan, R. S.; Garrison, J.; Bridge, D.; House, M.; Frye, M. S.; Loveless, B.; Norwood, D. *J. Clin. Microbiol.* **2004**, *42*, 179−185.
(4) King, D.; Luna, V.; Cannons, A.; Cattani, J.; Amuso, P. *J. Clin. Microbiol.* **2003**, *41*, 3454−3455.
(5) Zhang, X. Y.; Young, M. A.; Lyandres, O.; Van Duyne, R. P. *J. Am. Chem. Soc.* **2005**, *127*, 4484−4489.
(6) Yilmaz, M. D.; Hsu, S. H.; Reinhoudt, D. N.; Velders, A. H.; Huskens, J. *Angew. Chem., Int. Ed.* **2010**, *49*, 5938−5941.
(7) Rosen, D. L.; Sharpless, C.; McGown, L. B. *Anal. Chem.* **1997**, *69*, 1082−1085.
(8) Pellegrino, P. M.; Fell, N. F., Jr.; Rosen, D. L.; Gillespie, J. B. *Anal. Chem.* **1998**, *70*, 1755−1760.
(9) Cable, M. L.; Kirby, J. P.; Sorasaenee, K.; Gray, H. B.; Ponce, A. *J. Am. Chem. Soc.* **2007**, *129*, 1474−1475.
(10) Ai, K.; Zhang, B.; Lu, L. *Angew. Chem., Int. Ed.* **2009**, *48*, 304−308.
(11) Ma, B. L.; Zeng, F.; Zheng, F. Y.; Wu, S. Z. *Analyst* **2011**, *136*, 3649−3655.
(12) Tan, C. L.; Wang, Q. M.; Zhang, C. C. *Chem. Commun.* **2011**, *47*, 12521−12523.
(13) Oh, W.-K.; Jeong, Y. S.; Song, J.; Jang, J. *Biosens. Bioelectron* **2011**, *29*, 172−177.
(14) Xu, H.; Rao, X. T.; Gao, J. K.; Yu, J. C.; Wang, Z. Q.; Dou, Z. S.; Cui, Y. J.; Yang, Y.; Chen, B. L.; Qian, G. D. *Chem. Commun.* **2012**, *48*, 7377−7379.
(15) Bailey, G. F.; Karp, S.; Sacks, L. E. *J. Bacteriol.* **1965**, *89*, 984−987.
(16) Goodacre, R.; Shann, B.; Gilbert, R. J.; Timmins, E. M.; McGovern, A. C.; Alsberg, B. K.; Kell, D. B.; Logan, N. A. *Anal. Chem.* **2000**, *72*, 119−127.
(17) Seveus, L.; Vaisala, M.; Hemmila, I.; Kojola, H.; Roomans, G. M.; Soini, E. *Microsc. Res. Tech.* **1994**, *28*, 149−154.
(18) Xiao, M.; Selvin, P. R. *J. Am. Chem. Soc.* **2001**, *123*, 7067−7073.
(19) Ma, B.; Zeng, F.; Zheng, F.; Wu, S. *Analyst* **2011**, *136*, 3649−3655.
(20) Wu, C.; Szymanski, C.; McNeill, J. *Langmuir* **2006**, *22*, 2956−2960.
(21) Wu, C.; Peng, H.; Jiang, Y.; McNeill, J. *J. Phys. Chem. B* **2006**, *110*, 14148−14154.
(22) Wu, C.; Szymanski, C.; Cain, Z.; McNeill, J. *J. Am. Chem. Soc.* **2007**, *129*, 12904−12905.
(23) Wu, C.; Bull, B.; Szymanski, C.; Christensen, K.; McNeill, J. *ACS Nano* **2008**, *2*, 2415−2423.
(24) Wu, C.; Bull, B.; Szymanski, C.; Christensen, K.; McNeill, J. *Angew. Chem., Int. Ed.* **2009**, *48*, 2741−2745.
(25) Wu, C.; Schneider, T.; Zeigler, M.; Yu, J.; Schiro, P.; Burnham, D.; McNeill, J. D.; Chiu, D. T. *J. Am. Chem. Soc.* **2010**, *132*, 15410−15417.
(26) Wu, C.; Chiu, D. T. *Angew. Chem., Int. Ed.* **2013**, *52*, 3086−3109.
(27) Wu, C.; Jin, Y.; Schneider, T.; Burnham, D. R.; Smith, P. B.; Chiu, D. T. *Angew. Chem., Int. Ed.* **2010**, *49*, 9436−9440.
(28) Wu, C.; Hansen, S.; Hou, Q.; Yu, J.; Zeigler, M.; Jin, Y.; Burnham, D.; McNeill, J.; Olson, J.; Chiu, D. T. *Angew. Chem., Int. Ed.* **2011**, *50*, 3430−3434.
(29) Ye, F. M.; Wu, C. F.; Jin, Y. H.; Chan, Y. H.; Zhang, X. J.; Chiu, D. T. *J. Am. Chem. Soc.* **2011**, *133*, 8146−8149.
(30) Chan, Y. H.; Wu, C. F.; Ye, F. M.; Jin, Y. H.; Smith, P. B.; Chiu, D. T. *Anal. Chem.* **2011**, *83*, 1448−1455.
(31) Chan, Y. H.; Jin, Y. H.; Wu, C. F.; Chiu, D. T. *Chem. Commun.* **2011**, *47*, 2820−2822.
(32) Childress, E. S.; Roberts, C. A.; Sherwood, D. Y.; LeGuyader, C. L. M.; Harbron, E. J. *Anal. Chem.* **2012**, *84*, 1235−1239.
(33) Pecher, J.; Mecking, S. *Chem. Rev.* **2010**, *110*, 6260−6279.
(34) Szymanski, C.; Wu, C.; Hooper, J.; Salazar, M. A.; Perdomo, A.; Dukes, A.; McNeill, J. D. *J. Phys. Chem. B* **2005**, *109*, 8543−8546.
(35) Parker, D.; Dickins, R. S.; Puschmann, H.; Crossland, C.; Howard, J. A. *Chem. Rev.* **2002**, *102*, 1977−2010.
(36) Wu, C.; McNeill, J. *Langmuir* **2008**, *24*, 5855−5861.
(37) Zhang, B. H.; Wang, H. S.; Lu, L. H.; Ai, K. L.; Zhang, G.; Cheng, X. L. *Adv. Funct. Mater.* **2008**, *18*, 2348−2355.
(38) Matz, L. L.; Beaman, T. C.; Gerhardt, P. *J. Bacteriol.* **1970**, *101*, 196−201.